Electronic Supplementary Material

Zeolitic imidazolate framework-based nanoparticles for the cascade enhancement of cancer chemodynamic therapy by targeting glutamine metabolism

Hui Jian[a, b], Yun Zhang[a, c]*, Junyue Wang[a, b], Zhenxiang Chen[a], Tingyi Wen[a, c, d]*

[a]CAS Key Laboratory of Pathogenic Microbiology and Immunology, Institute of Microbiology, Chinese Academy of Sciences, Beijing 100101, China

[b] University of Chinese Academy of Sciences, Beijing 100049, China

[c]Innovation Academy for Green Manufacture, Chinese Academy of Sciences, Beijing 100190, China

[d] Savaid Medical School, University of Chinese Academy of Sciences, Beijing 100049, China

*Corresponding author: Tingyi Wen, E-mail: wenty@im.ac.cn; Yun Zhang, E-mail: zhangyun@im.ac.cn.

1. Supplementary Methods

Untargeted metabolomics analysis

MDA-MB-231 cells (2×10^6) were seeded in T75 cell culture flasks and cultured for 4 h, and then exposed to PBS, CB-839 (2.3 μg mL^{-1}), ZIF(Fe) NPs (22.7 μg mL^{-1}) or ZIF(Fe)&CB NPs (25 μg mL^{-1}) for 24 h. After washing with precooled PBS three times, cells were collected in a clear cryopreservation tube by centrifugation and immediately frozen in liquid nitrogen. Each sample had six parallel replicates in the experiment.

All samples were removed from liquid nitrogen and slowly thawed at 4 °C for extraction of metabolites. An appropriate amount of cells in each group was resuspended in 1 mL pre-cooled methanol/acetonitrile/H_2O (2/2/1, v/v/v). The suspension was ultrasonicated for 30

min at 4 ℃, left standing at -20 ℃ for 10 min, and then centrifuged for 20 min at 14, 000 *g* and 4 ℃. The supernatant of all samples was subsequently recovered and dried in a vacuum centrifuge. For LC-MS analysis, the samples were redissolved in 100 μL of acetonitrile/water (1/1, v/v) solvent. To monitor the stability and repeatability of instrument analysis, quality control (QC) samples were prepared by pooling 10 μL of each sample and analyzed together with the other samples. The QC samples were regularly inserted and analyzed every 5 samples.

LC-MS/MS analyses were performed using a UHPLC (1290 Infinity LC, Agilent Technologies) coupled to a quadrupole time-of-flight (AB Sciex TripleTOF 6600) by Shanghai Applied Protein Technology Co., Ltd. (Shanghai, China). MS detection was performed in both positive and negative ionization modes.

The original UHPLC-QTOF-MS data (.wiff format) files were converted to the .mzXML format using ProteoWizard and then processed by XCMS software for peak alignment, retention time adjustment, and extraction of peak intensities. Metabolites were identified using accurate mass matching (< 25 ppm), secondary spectrum matching methods, and a search of the laboratory's self-built commercial database (Shanghai Applied Protein Technology Co. Ltd) using the annotation level (0-2) described by the metabolic standards initiative (MSI). After normalization to the total peak intensity, the processed data were uploaded before importing into SIMCA-P (version 14.1, Umetrics, Umea, Sweden), where they were subjected to multivariate data analysis, including Pareto-scaled principal component analysis (PCA), partial least-squares discriminant analysis (PLS-DA) and orthogonal partial least-squares discriminant analysis (OPLS-DA). Sevenfold cross-validation and response permutation testing were used to evaluate the robustness of the model. The variable importance in the projection (VIP) value of each variable in the OPLS-DA model was calculated to indicate its contribution to the classification. Significance was determined

using an unpaired Student's t test. OPLS-DA VIP value > 1 and *p* value < 0.05 were considered statistically significant.

For KEGG pathway annotation, the metabolites were blasted against the online Kyoto Encyclopedia of Genes and Genomes (KEGG, http://www.kegg.jp/) database to retrieve their COs and were subsequently mapped to pathways in KEGG. The corresponding KEGG pathways were extracted. To further explore the impact of differentially expressed metabolites, enrichment analysis was performed. KEGG pathway enrichment analyses were applied based on the Fisher's exact test, considering the whole metabolites of each pathway as a background dataset. Only pathways with *p* value < 0.05 were considered as significantly changed pathways.

2. Supplementary tables

Table S1. Liver and renal function assessment of mice after treatment with PBS, CB-839 (1.86 mg kg^{-1} mice), ZIF(Fe) NPs (18.14 mg kg^{-1} mice), and ZIF(Fe)&CB NPs (20 mg kg^{-1} mice). The data are presented as the mean ± SD (n = 5). Liver function: ALP, alkaline phosphatase; GGT, gamma-glutamyl transpeptidase; ALB, albumin. Renal function: BUN, blood urea nitrogen; CREA, creatinine; UA, uric acid.

Parameters / Groups	ALP ($U\ L^{-1}$)	GGT ($U\ L^{-1}$)	ALB ($g\ L^{-1}$)	BUN ($mg\ dL^{-1}$)	CREA ($\mu mol\ L^{-1}$)	UA ($\mu mol\ L^{-1}$)
Healthy mice	40 ± 7	4.0 ± 1.3	17.0 ± 1.1	14.2 ± 1.9	62 ± 26	180.1 ± 1.2
PBS	35 ± 9	3.7 ± 0.6	15.9 ± 2.9	12.0 ± 3.3	71 ± 30	179.5 ± 68.2
ZIF(Fe)	41 ± 11	4.9 ± 1.5	16.2 ± 1.7	12.4 ± 2.3	62 ± 40	162.9 ± 42.0
CB-839	42 ± 18	3.4 ± 1.5	17.1 ± 0.6	15.7 ± 1.4	71 ± 17	182.4 ± 29.9
ZIF(Fe)&CB	40 ± 15	4.3 ± 1.5	15.3 ± 1.3	14.1 ± 4.6	60 ± 17	168.8 ± 31.9

Table S2. Quantification of blood ions of mice after treatment with PBS, CB-839 (1.86 mg kg^{-1} mice), ZIF(Fe) NPs (18.14 mg kg^{-1} mice), and ZIF(Fe)&CB NPs (20 mg kg^{-1} mice). The data are presented as the mean ± SD (n = 5).

Parameters / Groups	Ca (mmol L^{-1})	K (mmol L^{-1})	P (mmol L^{-1})	Fe (mmol L^{-1})	Zn (mmol L^{-1})	Cl (mmol L^{-1})
Healthy mice	2.17 ± 0.03	2.98 ± 1.11	1.70 ± 0.21	25 ± 9	14.9 ± 0.2	138.2 ± 4.3
PBS	2.16 ± 0.04	3.08 ± 0.46	1.60 ± 0.36	26 ± 9	14.5 ± 1.0	141.3 ± 5.7
ZIF(Fe)	2.18 ± 0.03	3.48 ± 1.17	1.67 ± 0.30	26 ± 9	14.4 ± 0.9	138.9 ± 4.8
CB-839	2.13 ± 0.02	3.66 ± 0.28	1.92 ± 0.11	28 ± 4	15. 0 ± 1.9	136.7 ± 1.0
ZIF(Fe)&CB	2.12 ± 0.01	3.63 ± 0.71	1.63 ± 0.33	30 ± 10	15.0 ± 1.3	139.8 ± 3.4

3. Supplementary Figures

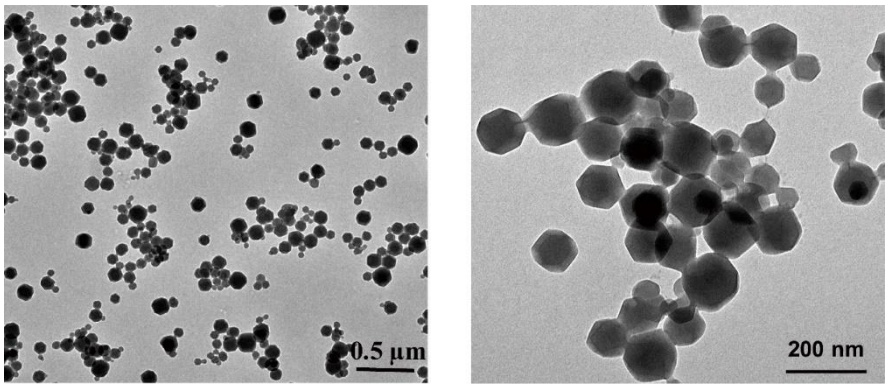

Fig. S1 TEM images of ZIF-8 nanoparticles.

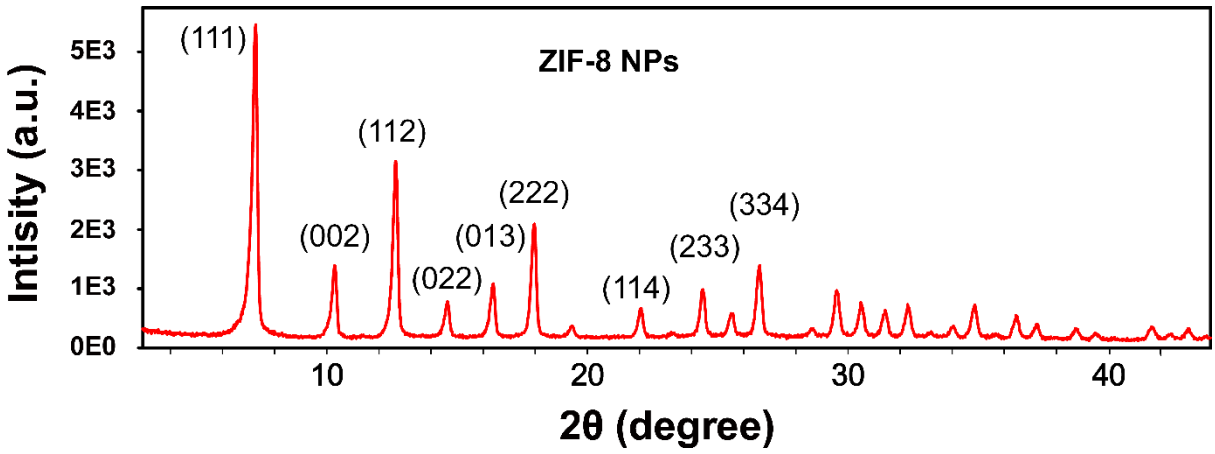

Fig. S2 X-ray diffraction (XRD) patterns of ZIF-8 nanoparticles.

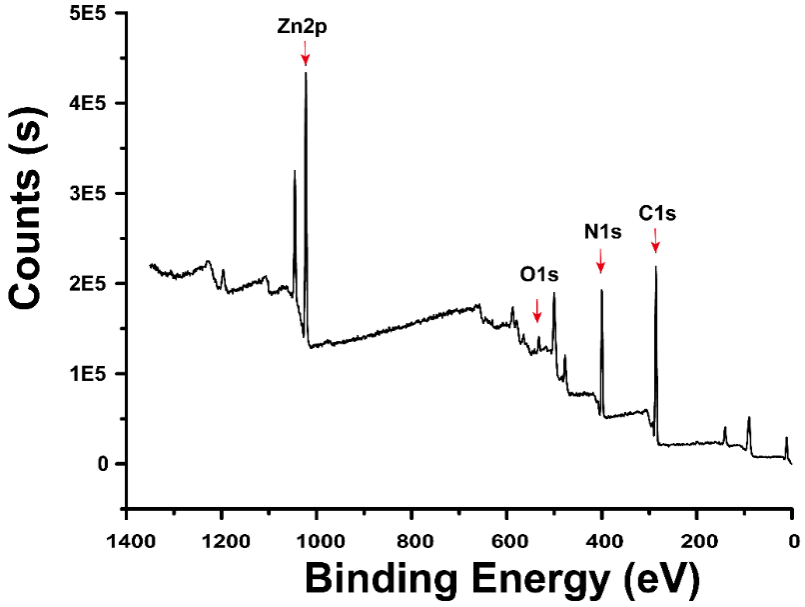

Fig. S3 X-ray photoelectron spectroscopy (XPS) survey spectra of ZIF-8 nanoparticles.

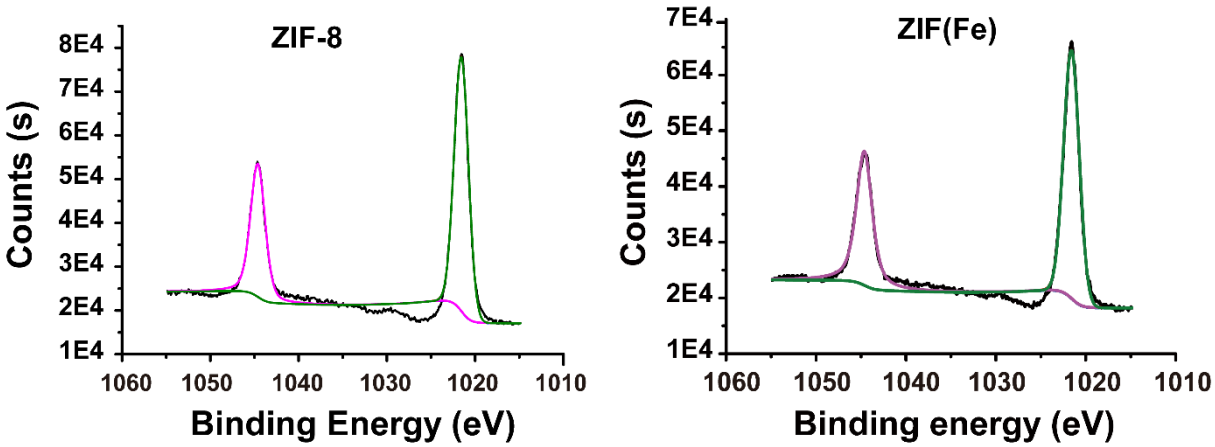

Fig. S4 High resolution Zn 2p XPS spectra of ZIF-8 and ZIF(Fe) nanoparticles.

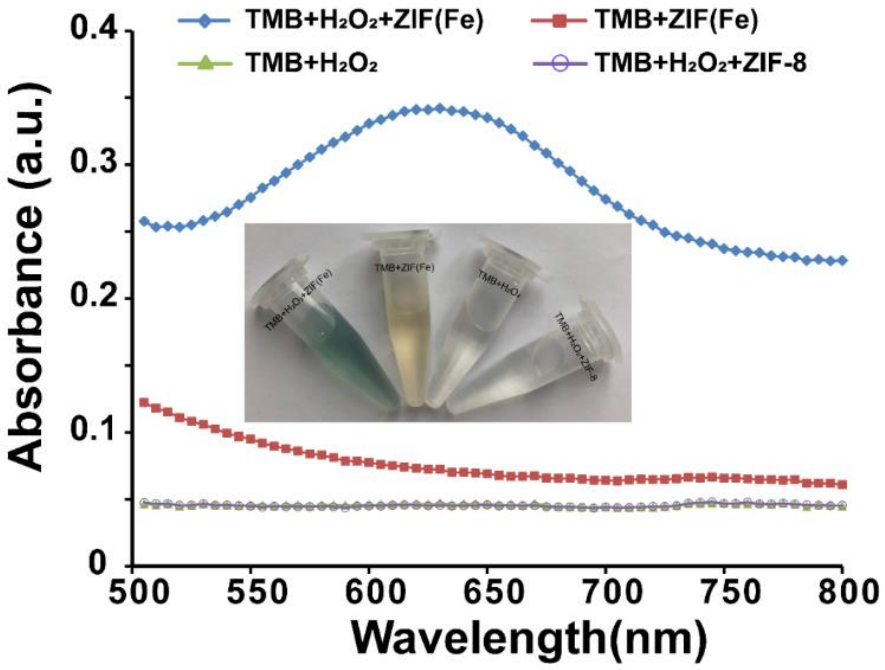

Fig. S5 *In vitro* characterizations of the Fenton catalytic performances of ZIF(Fe) nanoparticles with UV-vis absorption spectra and color change (inset) of TMB.

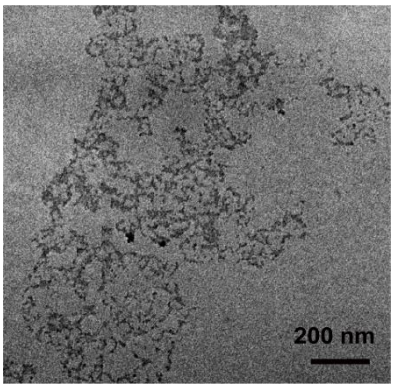

Fig. S6 TEM images of ZIF(Fe)&CB NPs after incubation in acetate buffer (pH = 5.0) for 2 h. Scale bar = 200 nm.

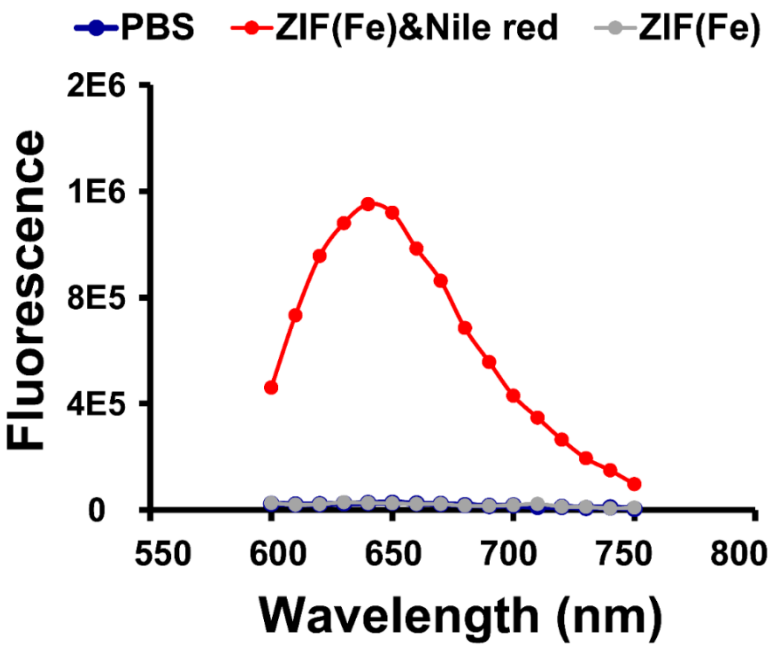

Fig. S7 Fluorescence absorption spectra of ZIF(Fe)&Nile red nanoparticles.

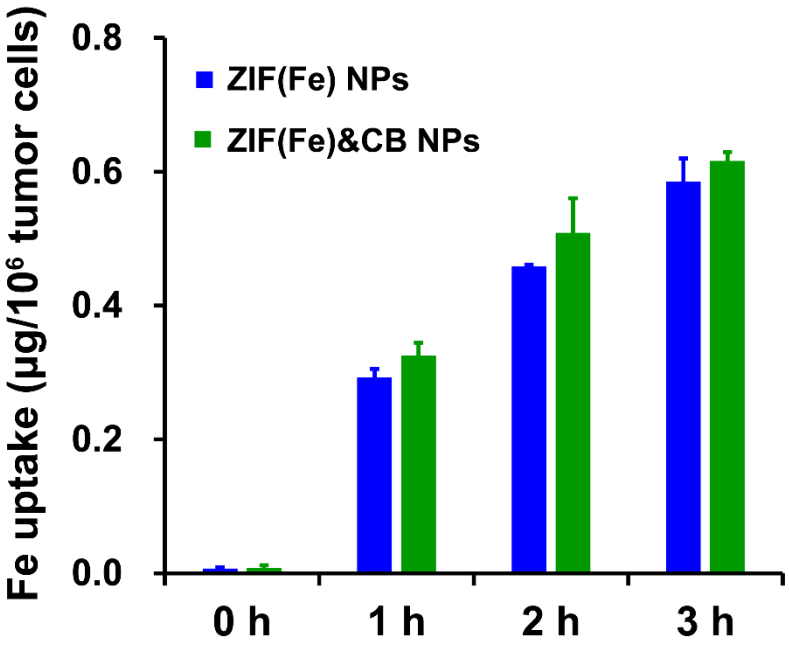

Fig. S8 Cellular uptake of Fe by MDA-MB-231 cells after treatment with ZIF(Fe) NPs (27.2 μg mL^{-1}) and ZIF(Fe)&CB NPs (30 μg mL^{-1}) for 0, 1, 2 and 3 h, respectively. All data are represented as the mean ± SD based on three parallel independent tests.

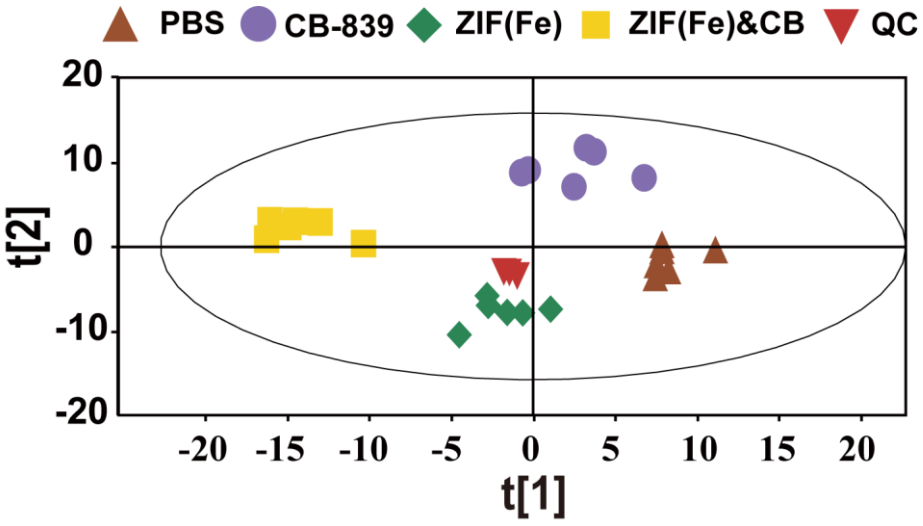

Fig. S9 PLS-DA score plot of metabolic profiles. Quality control (QC) samples were prepared by pooling 10 μL of each sample and analyzed together with the other samples. The QC samples were regularly inserted and analyzed every 5 samples.

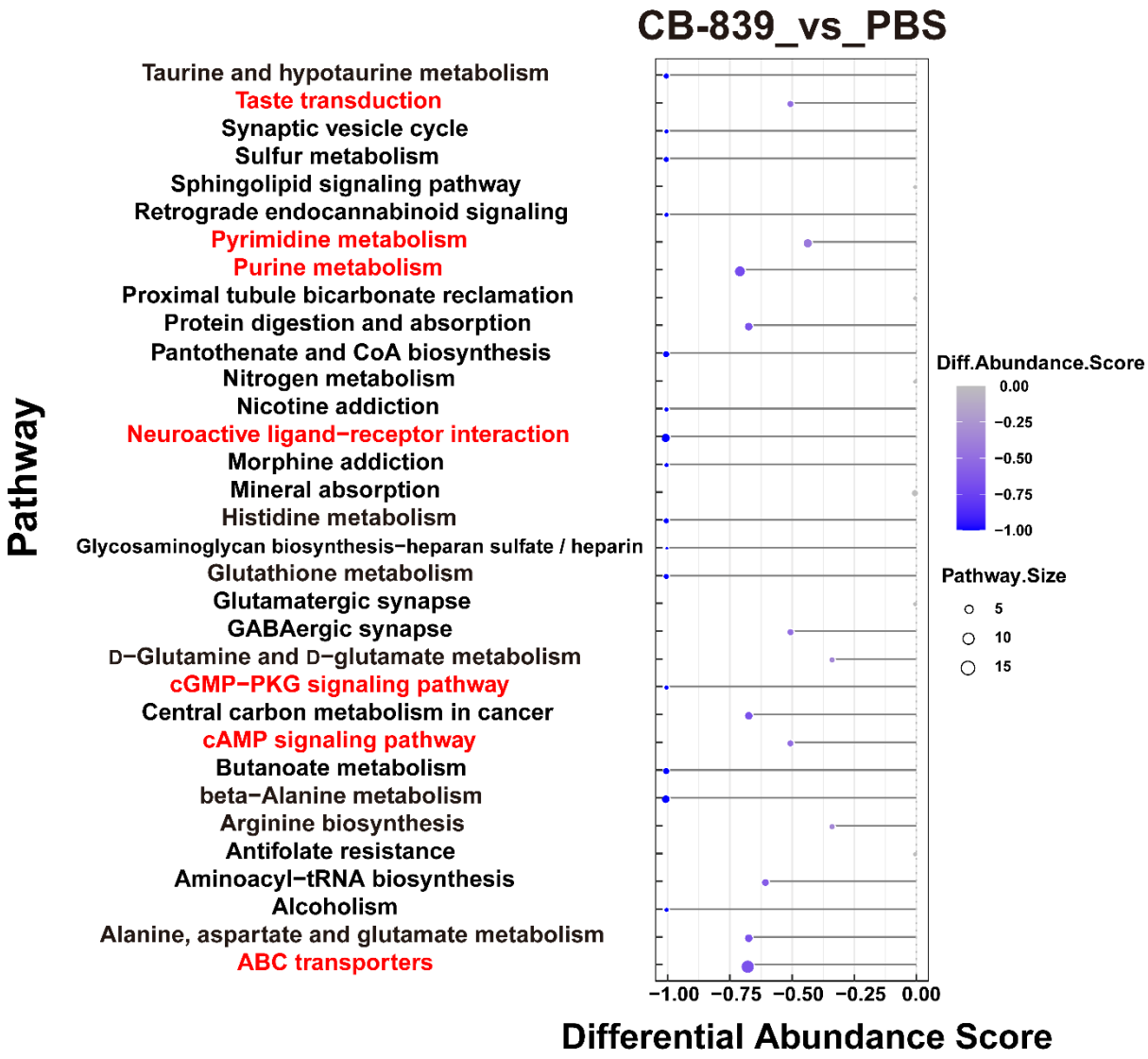

Fig. S10 KEGG pathway enrichment analysis of significantly changed metabolites in CB-839-treated MDA-MB-231 cells. Only significantly differential metabolic pathways with a *p* value < 0.05 (Fisher's exact test) are listed.

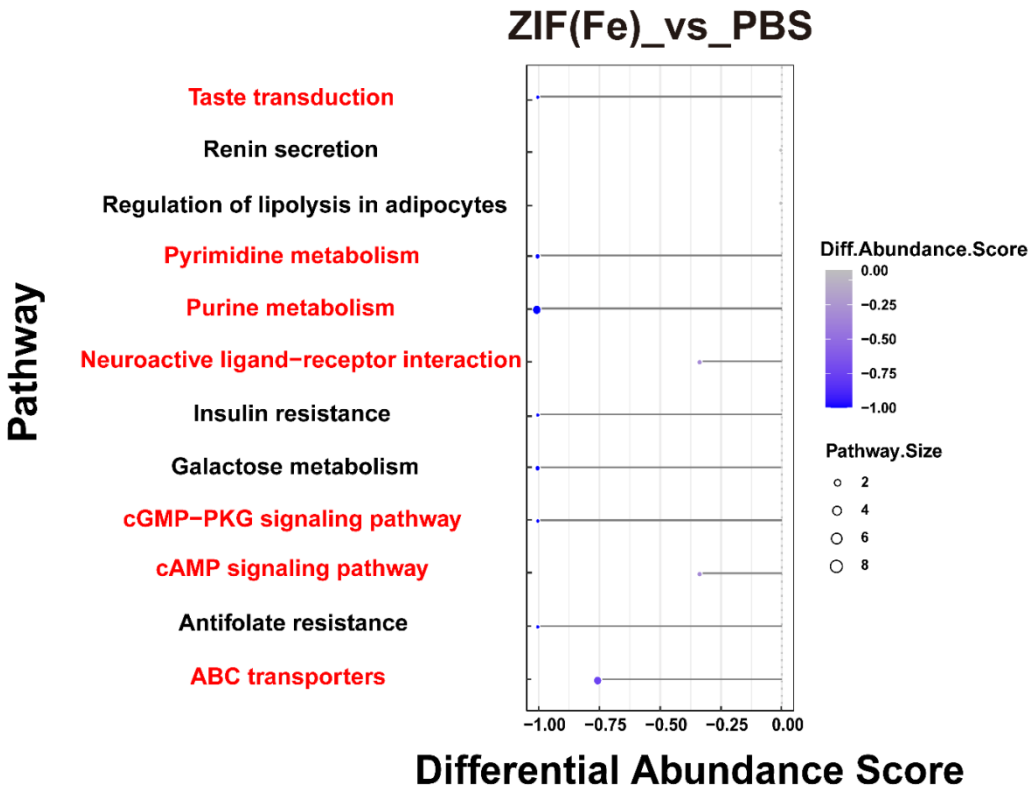

Fig. S11 KEGG pathway enrichment analysis of significantly changed metabolites in ZIF(Fe) NP-treated MDA-MB-231 cells. Only significantly differential metabolic pathways with a *p* value < 0.05 (Fisher's exact test) are listed.

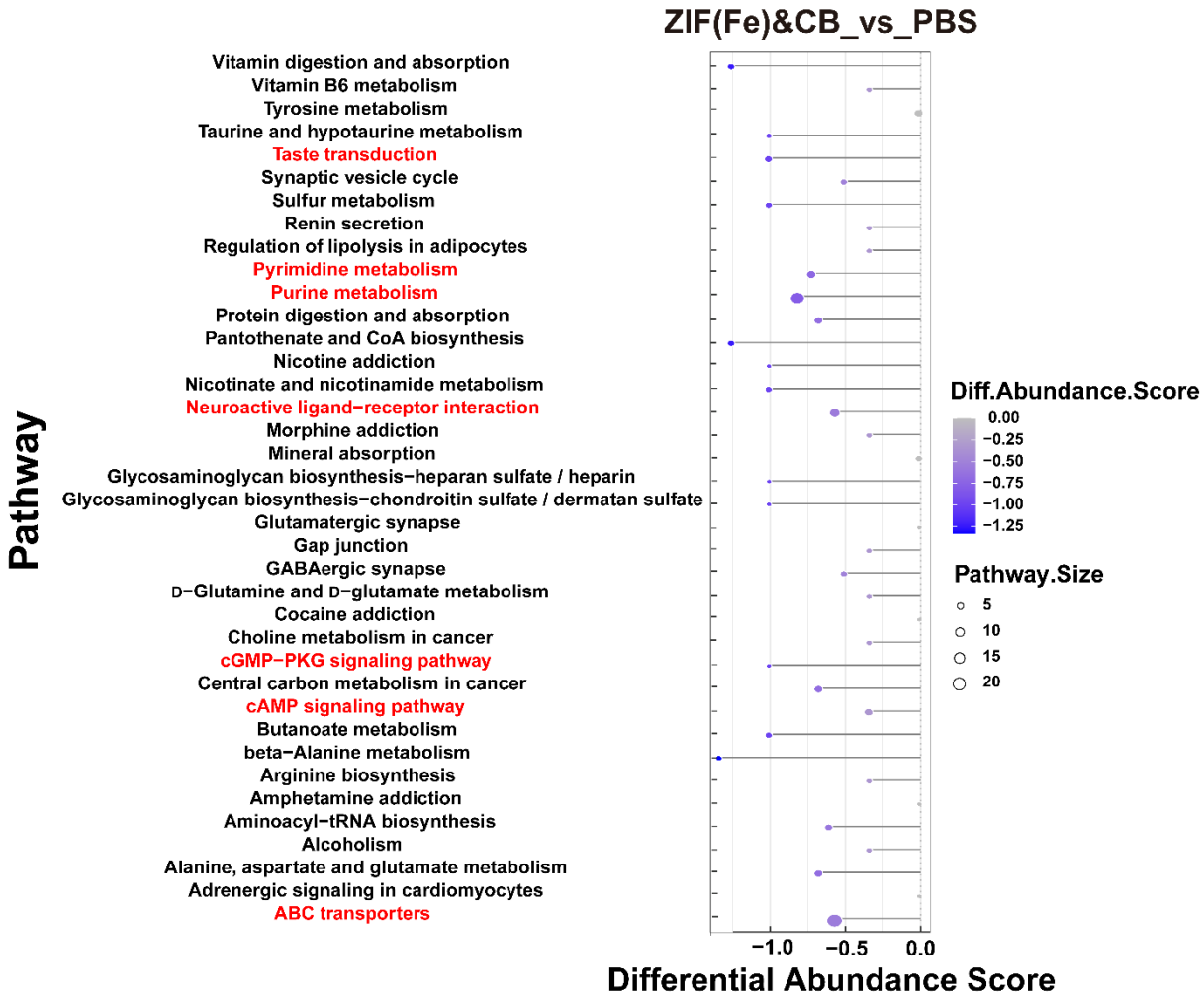

Fig. S12 KEGG pathway enrichment analysis of significantly changed metabolites in ZIF(Fe)&CB NP-treated MDA-MB-231 cells. Only significantly differential metabolic pathways with a *p* value < 0.05 (Fisher's exact test) are listed.

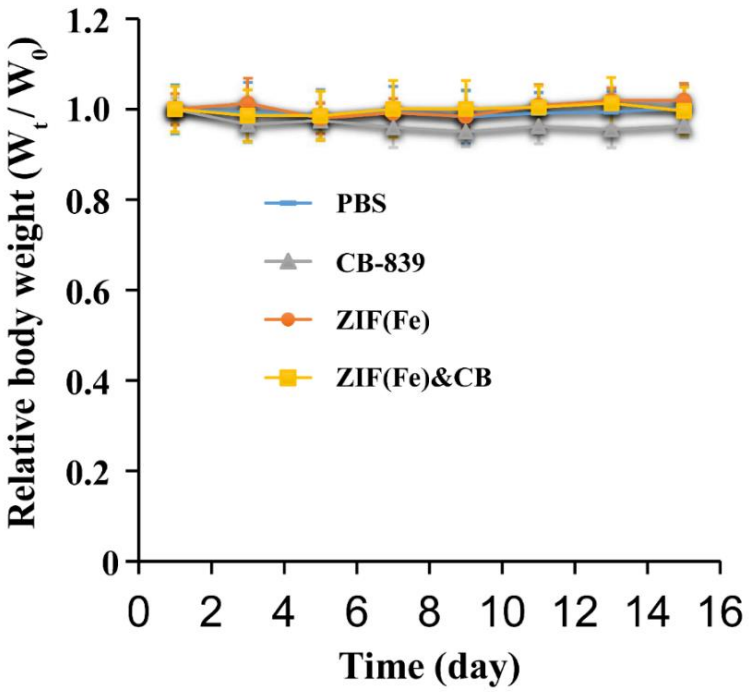

Fig. S13 The relative body weights of mice during treatment with PBS, CB-839 (1.86 mg kg^{-1} mice), ZIF(Fe) NPs (18.14 mg kg^{-1} mice), and ZIF(Fe)&CB NPs (20 mg kg^{-1} mice) (n = 5). All data are represented as the mean ± SD.

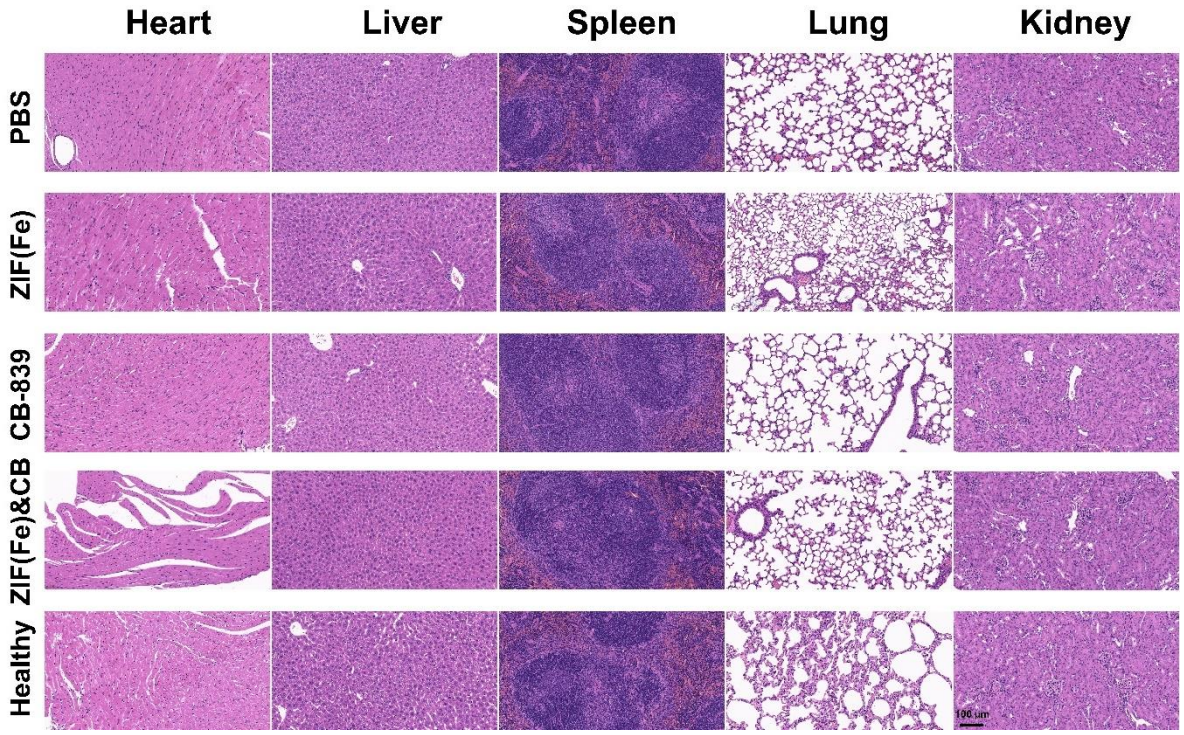

Fig. S14 Histopathology images of major organs of mice (n = 5) after treatment with PBS, CB-839 (1.86 mg kg^{-1} mice), ZIF(Fe) NPs (18.14 mg kg^{-1} mice), and ZIF(Fe)&CB NPs (20 mg kg^{-1} mice). Scale bar = 100 μm.

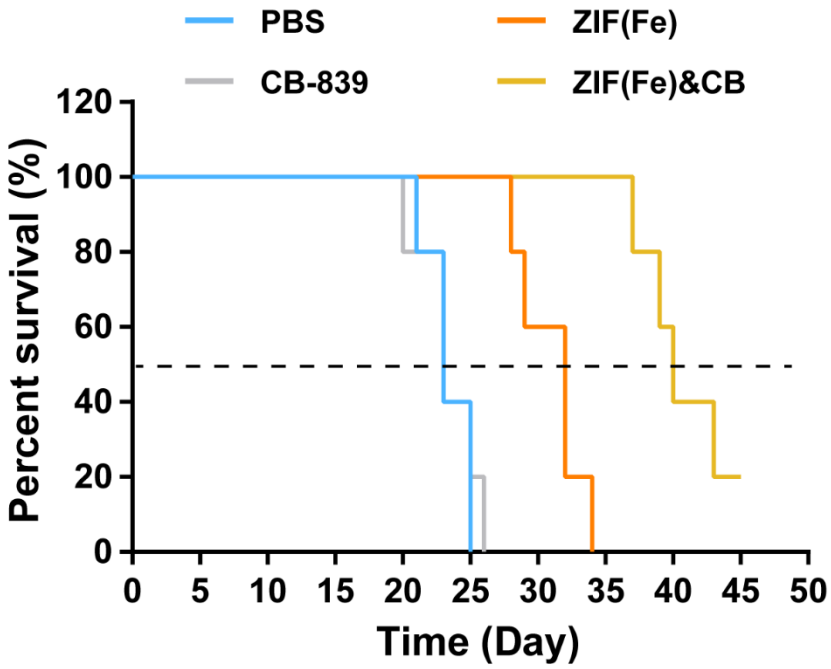

Fig. S15 Survival rate of mice (n = 5) after treatment with PBS, CB-839 (1.86 mg kg^{-1} mice), ZIF(Fe) NPs (18.14 mg kg^{-1} mice), and ZIF(Fe)&CB NPs (20 mg kg^{-1} mice).